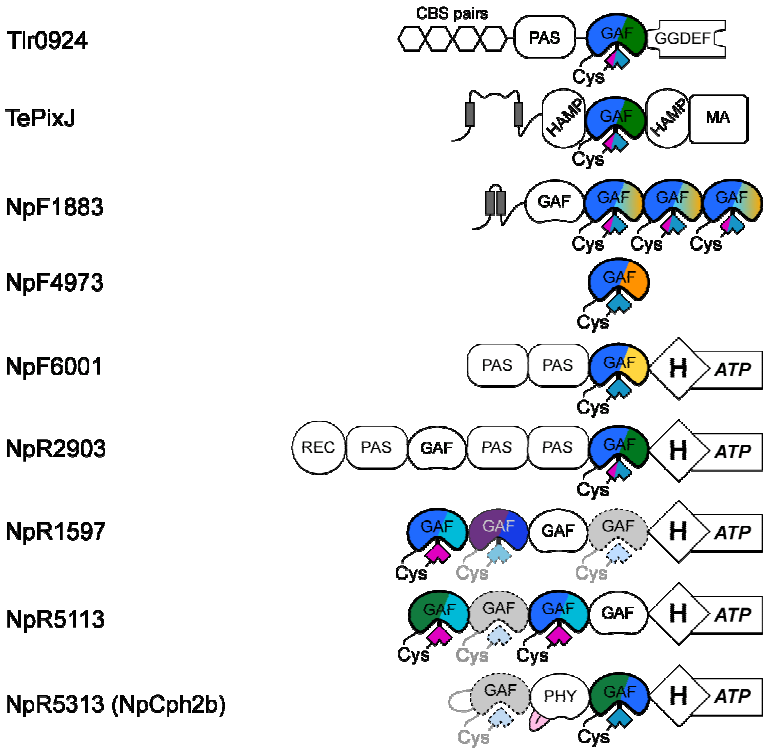

Figure S1. Domain structures of DXCF CBCRs examined in this study. CBCRs are outlined in thick black lines and color-coded by photocycle. The polygon below the GAF domain represents the bilin (blue, PCB; pink, PVB; blue/pink mix, PCB/PVB mix). H-ATP, histidine kinase module; MA, methyl-accepting chemotaxis domain; REC, response regulator receiver domain; HAMP, linker domain (found in Histidine kinases, Adenylate cyclases, Methyl-accepting proteins and Phosphatases); GGDEF, domain named for conserved motif and implicated in metabolism of the bacterial second messenger cyclic-di-GMP.

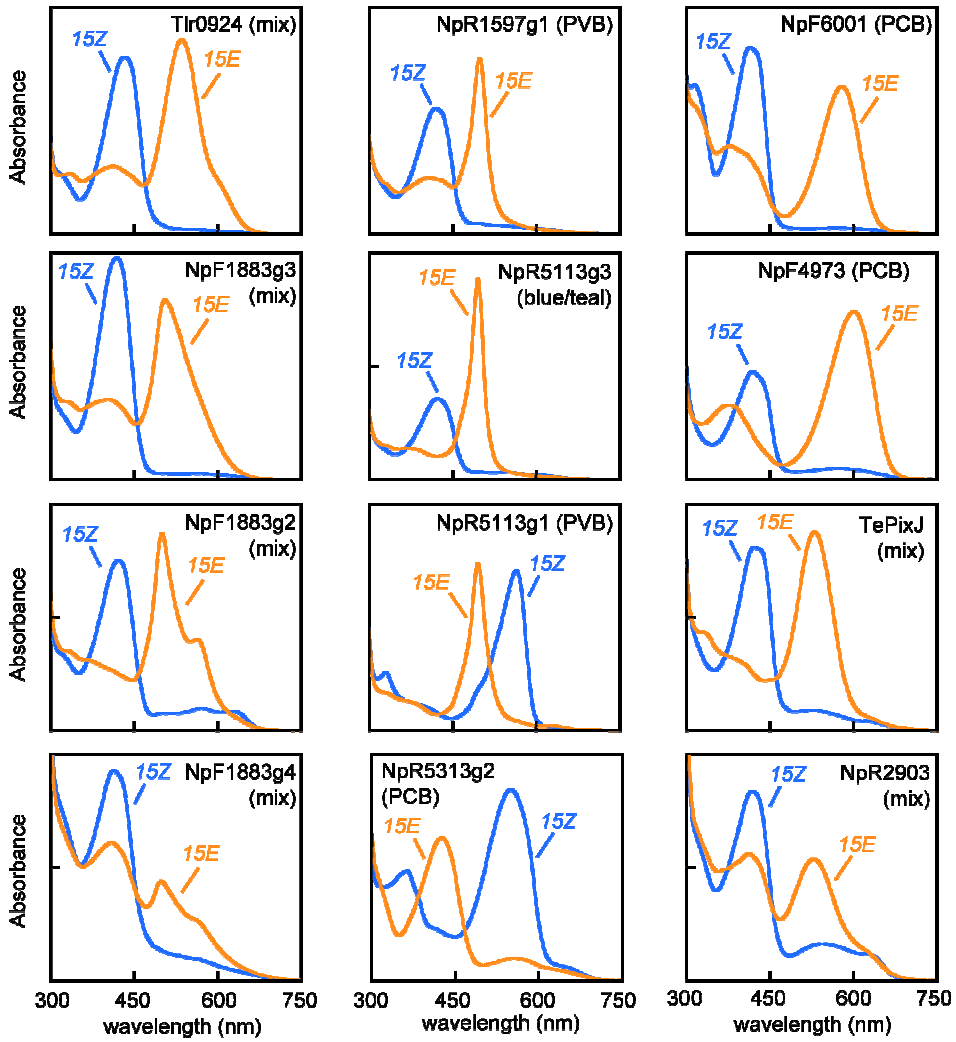

Figure S2. Photocycles of DXCF CBCRs used in this study. Protein name and bilin composition are indicated. Data are taken from Ref. (*1*).

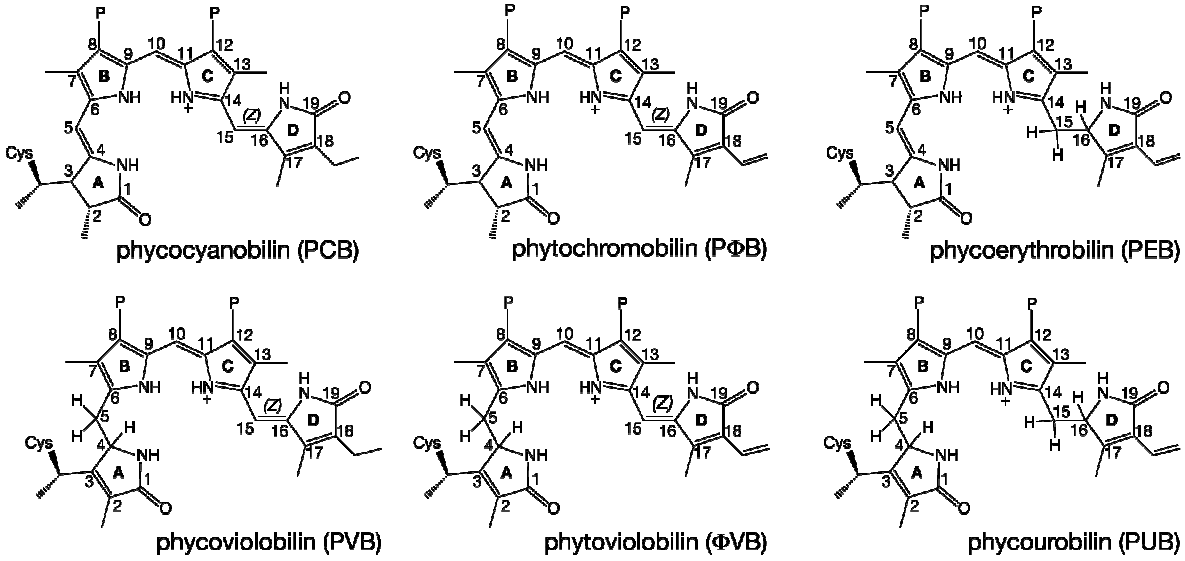

Figure S3. Bilin chromophores used in this study. Bilin chromophores are shown as covalent dark-state adducts in the 15-*Z,anti* configuration. Relative to PCB, PΦB and PEB both have vinyl moieties at C18 instead of ethyl, while PEB also has a reduced 15,16 bond. PVB has a reduced 4,5 bond but an oxidized 2,3 bond, while PUB has the isomerization seen in PEB and that seen in PVB. Therefore, PCB, PVB, PEB, and PUB are all at the same oxidation state. ΦVB is the 18-vinyl analog of PVB, and hence is at the same oxidation state as PΦB.

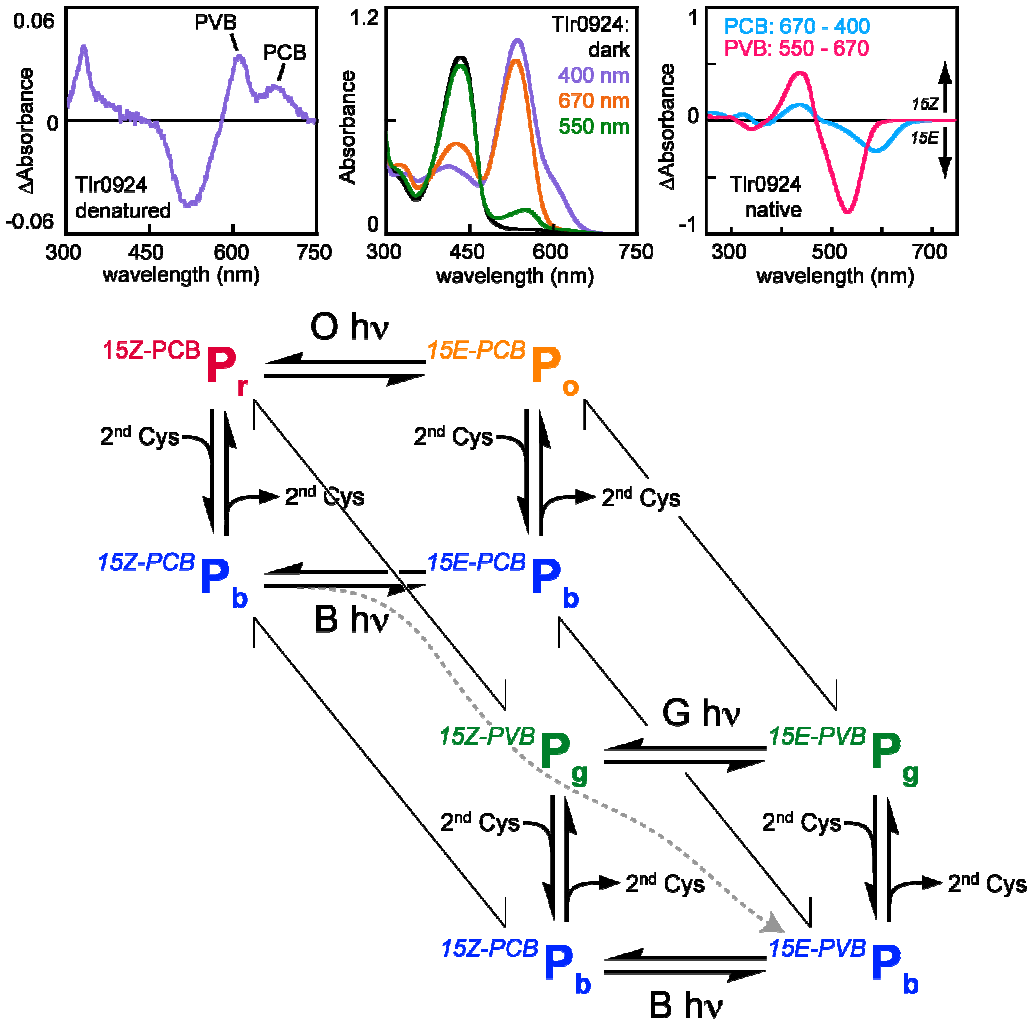

Figure S4. Parallel photocycles in DXCF CBCRs with mixed bilins. Mixed bilin populations can be detected by examining the photochemical difference spectrum of acid-denatured *15E* samples (top left). It can also be detected by sequential reverse photoconversion (top center), resulting in difference spectra for the two native populations (top right). Data are from (*1*). (B) Such mixed cases result in parallel photocycles, with slow isomerization between PCB and PVB. Direct photochemical isomerization between PCB and PVB (dashed grey line) is only shown for one case for clarity, but such reactions are formal possibilities for all photochemical steps.

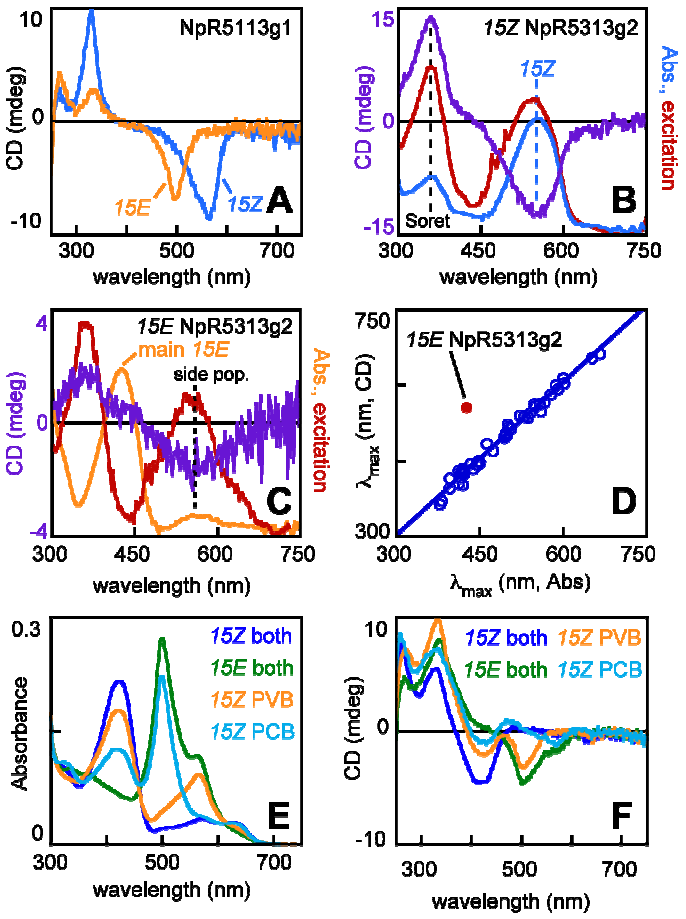

Figure S5. CD spectra of native DXCF CBCRs. (A) CD spectra are shown for NpR5113g1 in the *15Z* (blue) and *15E* (orange) states. (B) Simultaneously recorded absorbance (blue), CD (purple), and fluorescence excitation (red) spectra are shown for *15Z* NpR5313g2. The green-absorbing band and Soret transition are shown. (C) Simultaneously recorded absorbance (orange), CD (purple) and excitation (red) spectra are shown for *15E* NpR5313g2. The main absorbance band is indicated, as is a side population that gives rise to the observed CD and fluorescence signals. (D) For recently characterized CBCRs (Refs. (*1-3*) and this work), peak wavelengths from CD spectra are plotted against peak wavelengths from absorbance spectra. Overall agreement is good, with the data fit by linear regression (slope = 1.0; intercept = -1.8; r^2 = 0.985). The poor agreement observed with *15E* NpR5313g2 is exceptional. (E) NpF1883g2 is shown in the dark state (dark blue), photoproduct state (green), with *15Z* PVB and *15E* PCB (orange), and with *15E* PVB and *15Z* PCB (teal). The orange spectrum was generated by brief illumination of the photoproduct with 500±20 nm light, permitting kinetic control of the reaction but stopping short of photoequilibrium to avoid reverse photoconversion of PCB. Other spectra were prepared using sequential reverse photoconversion (*1*). (F) CD spectra are shown for the states of NpF1883g2 shown in panel E, using the same color scheme.

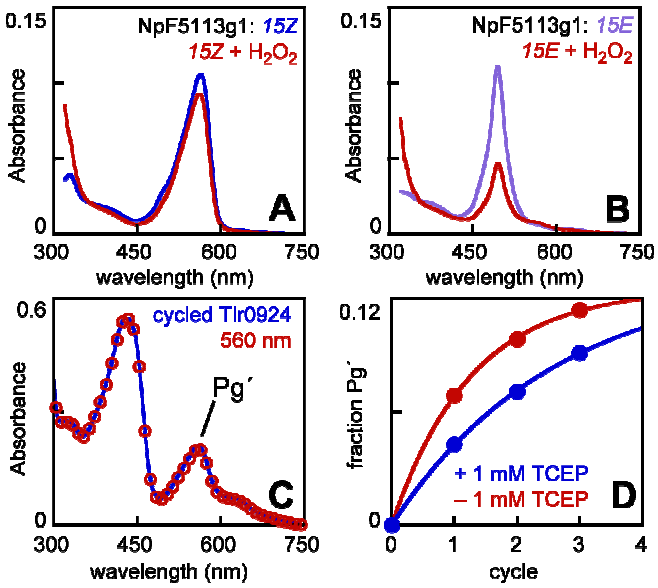

Figure S6. Chemical modification of DXCF CBCRs with oxidative reagents. (A) H_2O_2 treatment of *15Z* NpR5113g1 produces no red shift. (B) H_2O_2 treatment of *15E* NpR5113g1 results in bleaching of the teal-absorbing photoproduct but produces no red shift. (C) A green-absorbing species (P_g´ in Ref. (*4*)) accumulates in *15Z* Tlr0924 with repeated cycling (blue). Illumination with 560±5 nm light resulted in a superimposable spectrum (red circles), demonstrating that this species is photoinert. (D) P_g' formation is suppressed by the reductant tris-carboxyethyl-phosphine (TCEP). Formation of P_g' over several cycles was monitored and fit to a single exponential. Parameters are expected to be fluence-dependent; those measured under these conditions were k_{app} = 0.8 cycle^{-1} without TCEP and k_{app} = 0.4 cycle^{-1} with TCEP.

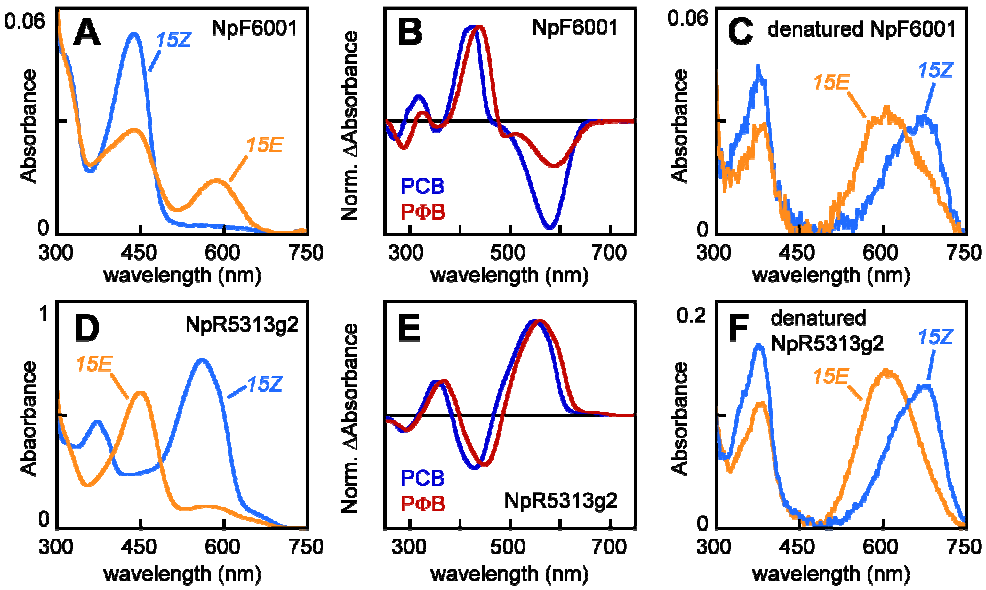

Figure S7. Characterization of the PΦB adducts of NpF6001 and NpR5313g2. (A) Absorbance spectra are shown for the PΦB adduct of NpF6001 in the *15Z* (blue) and *15E* (orange) states. (B) Normalized difference spectra are shown for the photoconversion of native NpF6001 with PCB (blue) or PΦB (red) adducts. (C) Absorbance spectra are shown for the acid-denatured PΦB adduct of NpF6001 in the color scheme of panel A. (D) Absorbance spectra are shown for the PΦB adduct of NpR5313g2 in the color scheme of panel A. (E) Normalized difference spectra are shown for the photoconversion of native NpR5313g2 in the color scheme of panel B. (F) Absorbance spectra are shown for the acid-denatured PΦB adduct of NpF6001 in the color scheme of panel A.

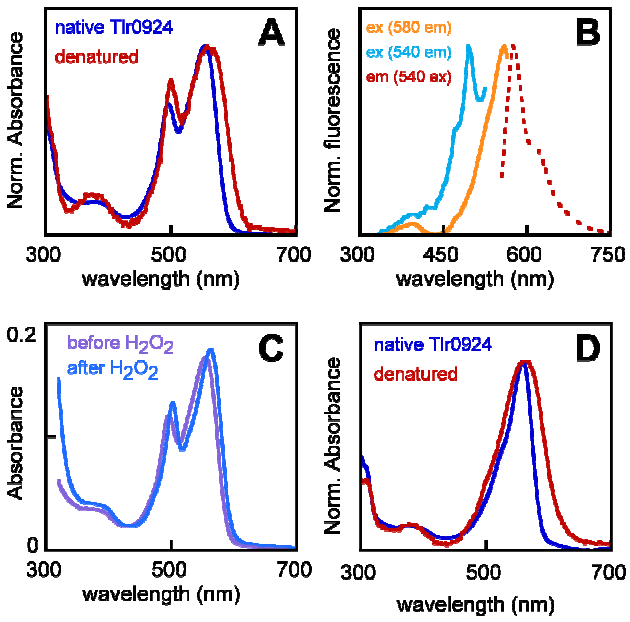

Figure S8. Formation of PUB by Tlr0924. (A) Normalized absorbance spectra are shown for native (blue) and acid-denatured (red) PEB adducts of Tlr0924 produced by co-expression with PEB (*1*). (B) Normalized fluorescence spectra are shown for the protein preparation in panel A. Orange, excitation spectrum with emission monitored at 580 nm (PEB). Teal, excitation spectrum with emission monitored at 540 nm (PUB). Red, emission spectrum with excitation at 540 nm (PEB). Emission from PUB was overlapped by PEB (not shown). (C) Absorbance spectra are shown for the protein preparation in panel A before (purple) and after (blue) treatment with peroxide. (D) Normalized absorbance spectra are shown for native (blue) and acid-denatured (red) PEB adducts of Tlr0924 produced by co-expression with PEB as described in the Methods. The minor PUB peak observed with co-expression is absent.

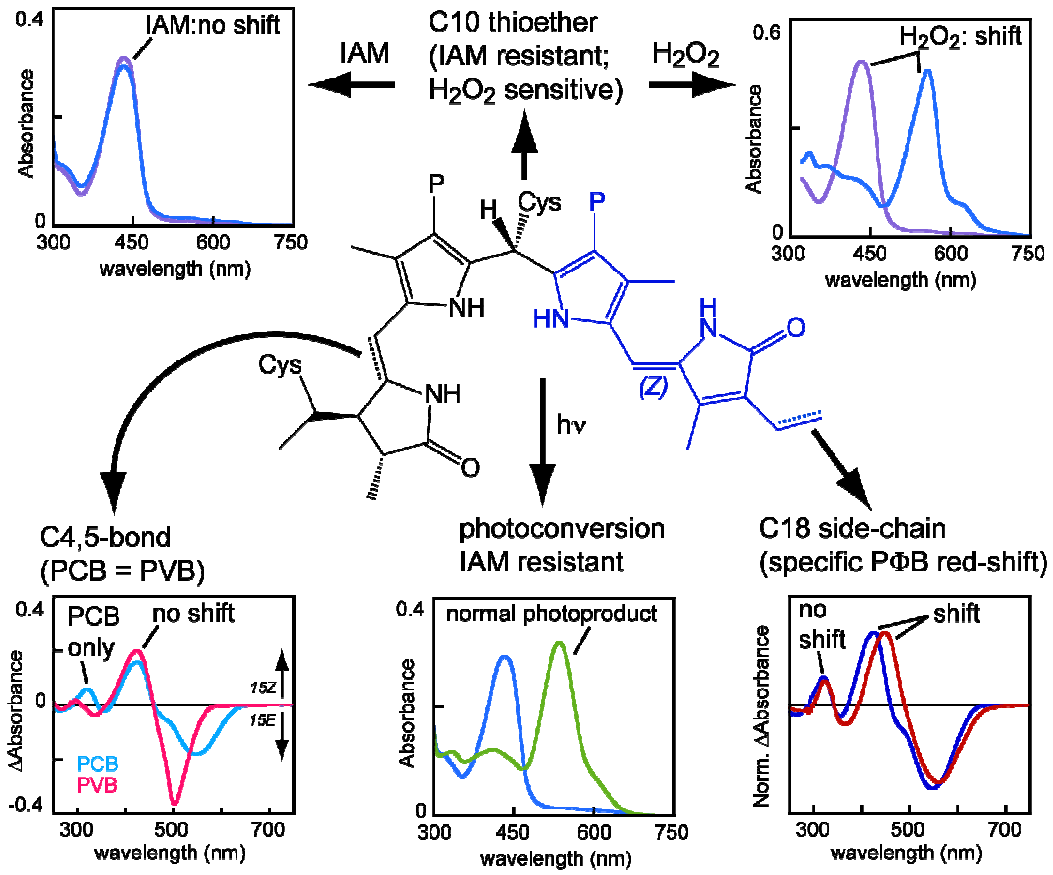

Figure S9. Mapping the conjugated system in dark states of Tlr0924 and NpF1883g3. In the *15Z* state, the PCB population is not red-shifted relative to the PVB population, and the second transition is only seen in PCB (bottom left). Desaturation of the C18 side-chain results in red shifts of only the first chromophore absorption band (bottom right). IAM does not shift the spectrum or prevent forward photoconversion (top left and bottom center), but H_2O_2 shifts dark-state absorption (top right). These results indicate a split-conjugated system at C10 (center). A similar scheme would apply to proteins with similar blue-absorbing dark states, such as NpF6001 or NpR1597g1.

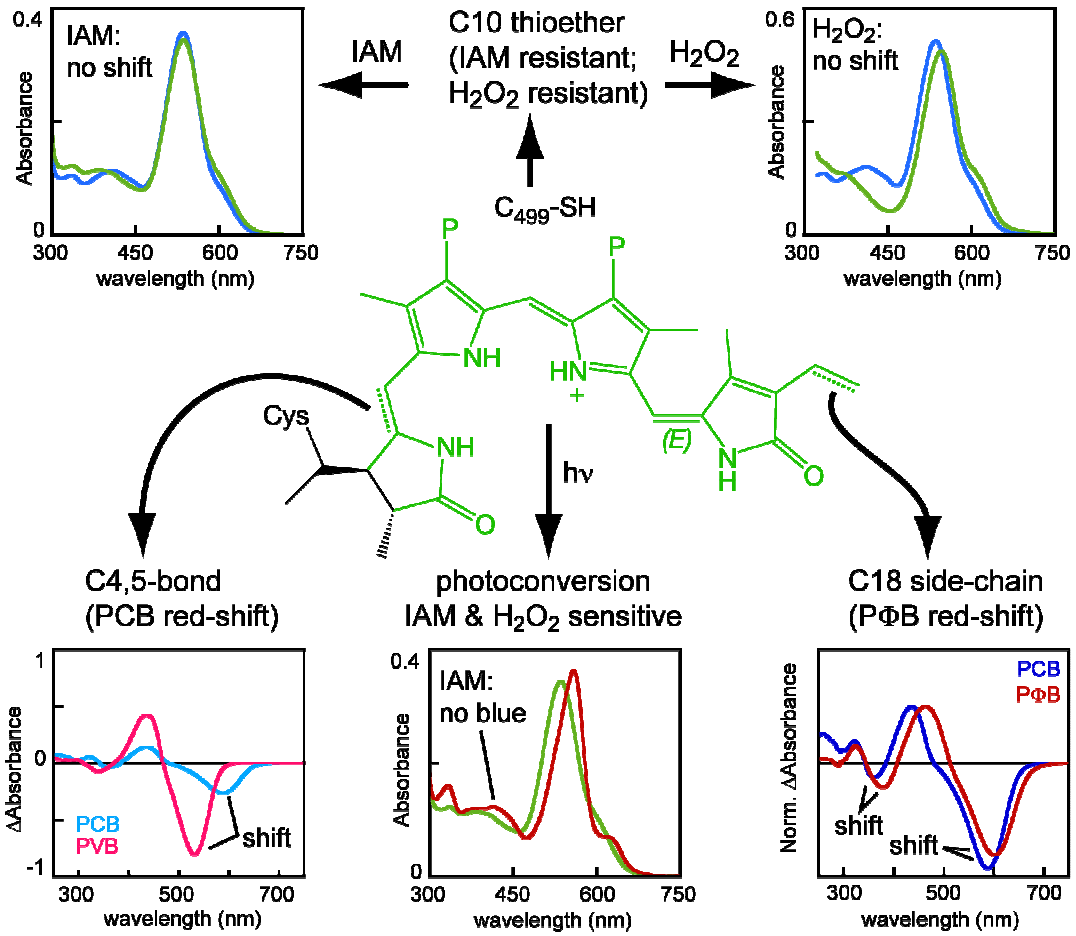

Figure S10. Mapping the conjugated system in photoproduct states of Tlr0924 and NpF1883g3. In the *15E* state, the PCB population is red-shifted relative to the PVB population (bottom left). Desaturation of the C18 side-chain results in red shifts of both resolved chromophore absorption bands (bottom right). Neither IAM nor H_2O_2 result in a shift of photoproduct absorption (top), but they prevent regeneration of the blue-absorbing ground state (bottom center). These results indicate a single conjugated system (center). A similar scheme would apply to proteins with similar photoproducts, such as NpF6001.

Table S1: Chromophore incorporation and C5 saturation of CBCRs[1]

Protein	bilin	native SAR	denatured SAR	C5 saturated:unsaturated
NpF6001	PCB	0.61	0.71	<< 1
NpF6001	PΦB	0.25	0.21	<< 1
NpR1597g1	PVB	0.40	0.46	≥ 10:1
NpR1597g1	ΦVB	0.17	0.14	≥ 10:1
NpR5113g1	PVB	0.31	0.23	≥ 10:1
NpR5113g1	ΦVB	~ 0.03	0.06	≥ 10:1
NpR5313g2	PCB	0.66	0.55	<< 1
NpR5313g2	PΦB	0.51	0.42	<< 1
NpF1883g3	PCB/PVB	0.42[2]	0.54[2]	1.2:1
NpF1883g3	PΦB/ΦVB	0.46[2]	0.44[2]	2.3:1
Tlr0924	PCB/PVB	0.49[2]	0.50[2]	2.9:1
Tr0924	PΦB/ΦVB	0.53[2]	0.38[2]	2.1:1

1. Specific absorbance ratio (SAR) was calculated by dividing the peak absorbance for the bilin transition at longest wavelength by that of the protein absorbance band in the near-UV. 4,5-saturation ratios are reported as saturated:unsaturated (PVB:PCB, etc.). Reversibility was calculated from forward and reverse difference spectra. Saturation ratios for mixed populations were calculated for the *15E* populations from the regenerated *15Z* spectra in sequential conversion assays, and values for PCB and PVB cases are from Ref. (*1*).

2. Reported for the mixed population.

REFERENCES FOR SUPPORTING INFORMATION

1. Rockwell, N. C., Martin, S. S., Gulevich, A. G., and Lagarias, J. C. (2012) Phycoviolobilin formation and spectral tuning in the DXCF cyanobacteriochrome subfamily, *Biochemistry 51,* 1449-1463.
2. Rockwell, N. C., Martin, S. S., Feoktistova, K., and Lagarias, J. C. (2011) Diverse two-cysteine photocycles in phytochromes and cyanobacteriochromes, *Proc. Natl. Acad. Sci. USA 108*, 11854-11859.
3. Kim, P. W., Freer, L. H., Rockwell, N. C., Martin, S. S., Lagarias, J. C., and Larsen, D. S. (2012) Femtosecond Photodynamics of the Red/Green Cyanobacteriochrome NpR6012g4 from Nostoc punctiforme. 1. Forward Dynamics, *Biochemistry 51*, 608-618.
4. Rockwell, N. C., Njuguna, S. L., Roberts, L., Castillo, E., Parson, V. L., Dwojak, S., Lagarias, J. C., and Spiller, S. C. (2008) A second conserved GAF domain cysteine is required for the blue/green photoreversibility of cyanobacteriochrome Tlr0924 from *Thermosynechococcus elongatus*, *Biochemistry 47*, 7304-7316.